SEGMENTATION OF OVERLAPPING CERVICAL CELLS: A VARIATIONAL METHOD WITH STAR-SHAPE PRIOR

Masoud S. Nosrati and Ghassan Hamarneh

Medical Image Analysis Lab, School of Computing Science
Simon Fraser University, BC, Canada
{smn6, hamarneh}@sfu.ca

ABSTRACT

Accurate and automatic detection and delineation of cervical cells are two critical precursor steps to automatic Pap smear image analysis and detecting pre-cancerous changes in the uterine cervix. To overcome noise and cell occlusion, many segmentation methods resort to incorporating shape priors, mostly enforcing elliptical shapes (e.g. [1]). However, elliptical shapes do not accurately model cervical cells. In this paper, we propose a new continuous variational segmentation framework with *star-shape* prior using directional derivatives to segment overlapping cervical cells in Pap smear images. We show that our star-shape constraint better models the underlying problem and outperforms state-of-the-art methods in terms of accuracy and speed.

Index Terms— Star-shape prior, cervical cell, segmentation, microscopy.

1. INTRODUCTION

According to the *World Cancer Report 2014*, cervical cancer is the fourth most common type of cancer in women. Fortunately, regular Pap smear screening allows for early detection and treatment of this type of cancer. Currently, Pap smear test is a manual screening procedure used to detect potentially pre-cancerous and cancerous regions in the endocervical canal of the female reproductive system.

Automatic segmentation of cervical cells in Pap smear images is a critical first step toward computer-aided diagnosis and automatic screening. The number and type of cervical cells (the latter typically inferred from features such as shape and area of cytoplasm and nucleus) are two important factors in detecting pre-cancerous changes in the uterine cervix. Therefore, accurate and automatic detection (or localization) and delineation (or segmentation) of such cells play critical roles in designing such automatic computer-aided diagnosis system. Due to the complexities of cell structures resulting from poor contrast and highly overlapping cells, the fast, accurate, and automatic cervical cell segmentation remains an open problem, despite recent advances [2, 3, 4, 5, 6].

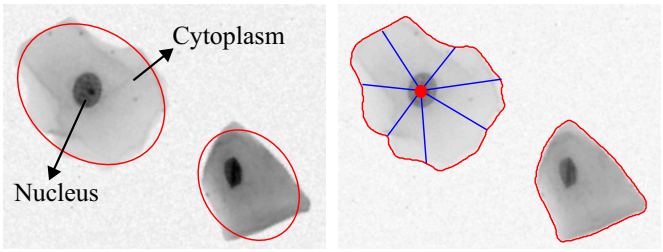

(a) Ellipsoid shape prior (b) star-shape prior

Fig. 1: Elliptical vs. star-shape prior. Star-shape prior (b) models cervical cells better than elliptical priors (a) used in [1].

Each cell in cervical cytology images consists of two parts: nucleus and cytoplasm. In the literature, some methods used parameter sensitive morphological operations to detect the nuclei [2]. However, they do not segment the cytoplasm which is a critical deficiency as the shape of the cytoplasm is an important property for the diagnosis. Other methods focused on segmenting free-lying (single non-overlapping) cells. For example, Yang et al. [3] and Li et al. [4] adopted gradient vector flow (GVF) snake to segment both the nucleus and cytoplasm of a single cell. Other works utilized unsupervised classification techniques to segment the nuclei and cytoplasm [5, 6]. However, these methods [5, 6] are not able to delineate the boundary of each individual overlapping cytoplasm. Instead, they segment the whole cell clump which is insufficient for subsequent cellular counting and shape analysis. Recently, Lu et al. [1] proposed a level sets-based method to segment nuclei and cytoplasm, simultaneously, of cervical cells. Their optimization energy functional consisted of several terms including regularization (length and area), elliptical shape prior, and two pairwise terms measuring the area overlap ratio and intensity ratio between neighbouring cells. As cervical cells are not exactly elliptical, adopting the elliptical shape prior cannot describe the segmentation problem very accurately (Fig. 1).

In this paper, we propose a new variational method to seg-

ment overlapping cervical cells. We show how to encode the *star-shape* prior into a continuous variational framework as a more general shape prior compared to the elliptical shape prior. The star-shape prior also better models the underlying segmentation problem unlike the elliptical shape prior used in [1] (Fig. 1). To handle the overlapping aspect of cervical cells, we introduce a Voronoi energy term which controls how much neighbouring cells can overlap. We validate our method on the dataset provided by the "Overlapping Cervical Cytology Image Segmentation Challenge" held in conjunction with the IEEE International Symposium on Biomedical Imaging (ISBI) 2014 and compare our method with the winners of this competition as well as the baseline method proposed by the challenge organizers [1].

2. METHODS

Given a cervical image $I : \Omega \subset \mathbb{R}^2 \rightarrow \mathbb{R}$, we are interested in segmenting each existing cell in the image. In cervical images, the nucleus typically stands out with high contrast (Fig. 1(a)). We take advantage of this feature and use nuclei as strong indicators of cells. Since a simple intensity thresholding alone is not enough to detect the nuclei in cervical images due to two reasons: 1) overlapping cytoplasms sometimes appear too dark and are mistaken for nuclei, and 2) nuclei may, albeit in rare cases, appear with low contrast and are confused with cytoplasm, we resort to a machine learning approach. We use the histogram of oriented gradient (HOG) features to represent the appearance of each nucleus and train a random decision forest (RF) consisting of T_n trees to detect the nuclei. Given a new image, rather than classifying every pixel in the image as nucleus vs. non-nucleus, we first reduce the search space for nuclei by applying bilateral filtering followed by the local thresholding technique proposed by Phansalkar et al. [7] and the circle Hough transform in order to *over-detect* the nuclei candidates. Then we apply the trained RF on these candidate locations to distinguish true from false nuclei. Next we describe how we segment the cytoplasm.

Let $u : \Omega \rightarrow \{0, 1\}$ be a labeling function such that $u(x) = 1$ if x belongs to the cytoplasm and $u = 0$ otherwise. To segment each cell, we propose the following energy functional:

$$E(u) = \lambda_1 E_S(u) + \lambda_2 E_V(u) + \lambda_3 E_R(u) + \mathcal{R}(u) \ , \quad (1)$$

where E_S is our star-shape prior term, E_v is the Voronoi energy term that controls how much cells are allowed to overlap, E_R is the regional data term, and $\mathcal{R}$ is the regularization term that ensures smooth segmentation boundaries. λ_1 to λ_3 are positive weights balancing the contribution of each term.

Star-shape prior. This type of shape prior is defined with respect to a center point c inside the object, which we set to be the centroid of the nucleus in our application. This prior was first introduced by Veksler in a discrete graph-cuts formulation [8]. According to [8], "an object has a star-shape if for any point x' inside the object, all points on the straight line between the center c and x' also lie inside the object" (Fig. 2(a)). In other words, in a star-shaped object, any ray from c cuts the object's boundary only once.

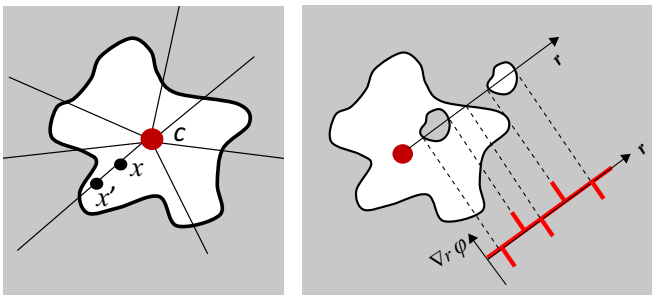

(a) (b)

Fig. 2: Star-shape definition and the directional derivative. (a) A star-shape example (with respect to c). (b) Directional derivative of u along the ray $\boldsymbol{r}$ used to enforce the star-shape.

Here, we show how an analogous star-shape prior can be encoded into our spatially continuous formulation. Let $\boldsymbol{r}$ be an outgoing ray from the detected nucleus of a cell (Fig. 2(b)). Since the transition from background to foreground along the ray $\boldsymbol{r}$ is an indication of the violation of the star-shape prior, we examine the gradient along $\boldsymbol{r}$, denoted as $\nabla_r u = \langle \nabla u, \boldsymbol{r} \rangle$. A positive gradient along $\boldsymbol{r}$ indicates a shape prior violation and must be penalized. So our energy term that favours star-shapes along each ray $\boldsymbol{r}$ is defined as $E_S(u) = \int_\Omega H(\nabla_r u(x))dx$ where $H(.)$ is the Heaviside function. As our derivative is along a radial ray, it is more convenient to re-formulate our problem using a polar coordinate system instead of a Cartesian system. Fig. 3 shows an example image unwrapped in a polar coordinate system around c. Defining $\Pi \subset \mathbb{R}^+ \times [0, 2\pi)$ as the polar-based image domain, the labeling function is re-written as $\nu : \Pi \rightarrow \{0, 1\}$ and our star-shape term becomes:

$$E_S(\nu) = \int_\Pi H(\nabla_r \nu(p))dp \ , \quad (2)$$

where $p \in \Pi$ and $\nabla_r \nu$ is the derivative of ν along the r-axis (Fig. 3).

Voronoi constraint. As the cervical cells overlap substantially (Fig. 4(a)), we allow cell segmentations to overlap as well. However, we define the Voronoi energy term (E_V) to limit excessive overlapping between neighbouring cytoplasm segmentations. Ushizima et al. [9] used a Voronoi diagram (Fig. 4(b)) to separate overlapping cells with a straight line which obviously is not realistic. Our energy (E_V) is a soft constraint allowing more realistic results. To define E_V, we first calculate the Voronoi diagram of the detected nuclei (Fig. 4(b)). Then, for each nucleus, we create a mask M that takes value 0 within the Voronoi cell of the current nucleus only and 1 otherwise (Fig. 4(c)). The purpose of this mask is to

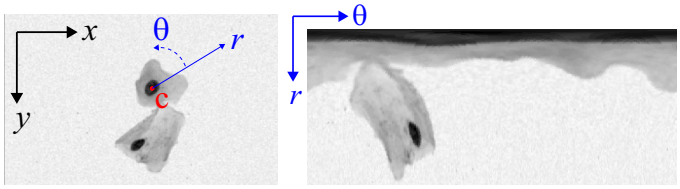

(a) (b)

Fig. 3: Cervical image in a Cartesian (a) and as polar (b) coordinate system defined around point c.

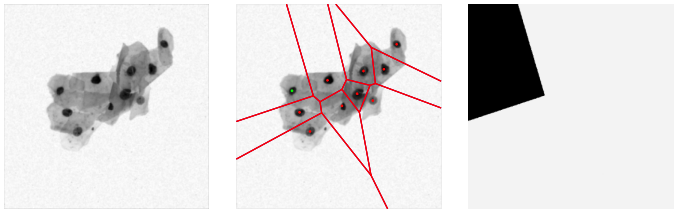

(a) (b) (c)

Fig. 4: Voronoi diagram for controlling the extent of cell overlap. (a) Overlapping cells. (b) Voronoi diagram of the detected nuclei (used as cell boundaries in [9]). (c) The mask M of all voronoi regions except the current cell's region.

counteract excessive cell overlap by penalizing the cytoplasm segmentation, of the current cell, as it extends farther from the nucleus. We define our Voronoi energy term in the Cartesian system as $E_V(u) = \int_\Omega u(x)M(x)dx$ to control the overlap between the current cell segmentation and its neighbouring regions. Finally, we re-write E_V in the polar system as:

$$E_V(\nu) = \int_\Pi \nu(p)\mu(p)dp \,, \tag{3}$$

where μ is the transformation of M to polar coordinates.

Regional term. Our regional term in the polar coordinate system is defined as:

$$E_R(\psi) = \int_\Pi g(p)\rho(p)\nu(p)dp \,, \tag{4}$$

where $g(.)$ is the polar-transformed version of $\frac{1}{1+|\nabla G_\sigma * I|}$, which encourages the evolving contours to align with edges. G_σ is a Gaussian kernel with standard deviation of σ. $\rho(p)$ is the regional term that measures the agreement of the image pixel $p \in \Pi$ with the background and cytoplasm statistical models and is calculated as follows

$$\rho(p) = \frac{\log\big(1 - Pr(p|I(p))\big)}{\log Pr(p|I(p))} \,, \tag{5}$$

where $Pr(p|I(p))$ is the probability of a given pixel p belonging to the foreground, i.e. cytoplasm. $Pr(p|I(p))$ is estimated by training a random forest with T_r trees using the provided ground truth segmentation in the training set.

Regularization term. Our regularization term in the polar coordinate system is defined as:

$$\mathcal{R}(\nu) = \int_\Pi |\nabla\nu(p)|dp \,. \tag{6}$$

$\mathcal{R}(\nu)$ regularizes the segmentation in both r and θ directions (Fig. 3). We re-write the energy functional (1) in polar coordinates as $E(\nu) = \lambda_1 E_S(\nu) + \lambda_2 E_V(\nu) + \lambda_3 E_R(\nu) + \mathcal{R}(\nu)$.

3. IMPLEMENTATION AND OPTIMIZATION

We used the level set function to represent the cells' boundary. In the Cartesian system, we represent $u(x)$ by $H(\phi(x))$ where $\phi : \Omega \to \mathbb{R}$ is a signed distance function such that $\phi(x) > 0$ for all x inside, $\phi(x) < 0$ for all x outside, and $\phi(x) = 0$ for all x on the boundary of the cytoplasm. Let $\psi : \Pi \to \mathbb{R}$ be the transformed level set from the Cartesian to the polar coordinate system. The energy terms (2)-(6) are written in terms of ψ by replacing ν and $\nabla_r\nu$ with $H(\psi)$ and $\nabla_r\psi$, respectively.

In our implementation, we approximate ∇_r by the finite forward differences, i.e. $\nabla_r u \approx u(x_2) - u(x_1)$ where x_2 and x_1 are two neighbouring points on the ray $\boldsymbol{r}$ and x_1 is between c and x_2.

We used $T_n = 40$ and $T_r = 48$ trees to train two random decision forests for detecting nuclei and learning the appearance prior of cytoplasm, respectively. Higher values of T_n and T_r did not improve accuracy but rather increased complexity and caused over-fitting to the training data. The weighting parameters were optimized on the 45 training images and fixed to $\lambda_1 = 1.5$, $\lambda_2 = 1$, and $\lambda_3 = 1.9$.

The objective energy functional in the polar coordinate system is optimized by deriving the Euler-Lagrange update equation. The final segmentation is obtained by transforming back the optimal ψ (or equivalently ν) from the polar to Cartesian coordinates.

4. MATERIALS AND EXPERIMENTS

We tested our method on the dataset provided by the ISBI 2014 challenge consisting of 135 cervical cytology images (45 images for training and 90 images for testing). The evaluation code provided by the challenge was used to evaluate the performance of our method on the test set.

Our nuclei detection approach (HOG features + RF) achieved the F1-value of 0.99 which is a great improvement in nuclei detection over a simple thresholding technique with F1-value of 0.88. Table I compares our method with state-of-the-art methods in overlapping cervical cell segmentation, including the winners of the ISBI 2014 challenge and Lu et al. [1]. Using the same notation as [1], in Table I we

Table 1: Quantitative results on the test sets (bold numbers indicates superior results).

	DSC	TP_p	FP_p	FNo	Time/Image	Computer specification
Ushizima [9]	0.87	0.83	**0.001**	0.17	12 sec.	Cray XC30 supercomputer, 12-core Intel, CPU 2.4 GHz, 64 GB RAM
Nosrati [10]	0.87	0.90	0.005	0.14	16.7 sec.	PC, CPU 3.40 GHz, 16 GB RAM
Lu [1]	**0.88**	0.92	0.002	0.21	1000.9 sec.	PC, CPU 2.7GHz , 40 GB RAM
Our method	**0.88**	**0.93**	0.005	**0.11**	**6.6 sec.**	PC, CPU 3.40 GHz, 16 GB RAM

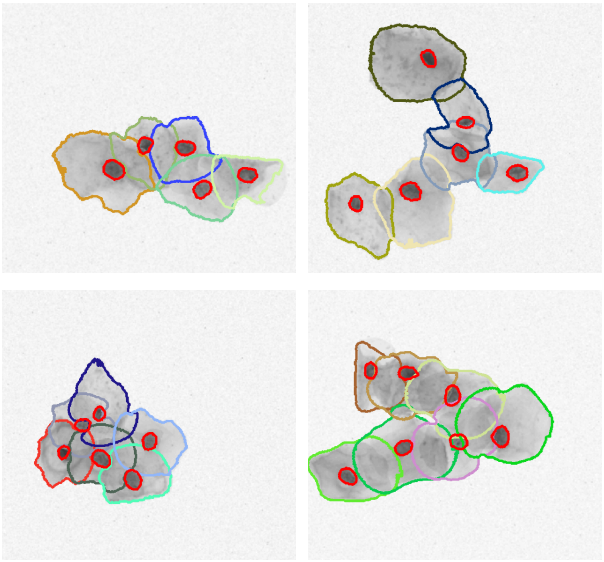

Fig. 5: Qualitative results of overlapping cervical cells segmentation.

report the Dice similarity coefficient (DSC), true positive (TP_p) and false positive (FP_p) ratio in the pixel level for "well-segmented" cells (segmented cells with $DSC > 0.7$). In addition, the false negative (FN_o) in the object level (inaccurate segmentation and/or missing cells) is reported as the proportion of cells having a $DSC \leq 0.7$. Fig. 5 shows qualitative results on some images in the test set. According to Table I, our method outperformed the recently proposed techniques in most of the criteria. Particularly, having a large advantage in FN_o compared with other methods confirms that our method has missed less cells and has estimated the cell boundaries much closer to the annotation of the detected cells. We emphasize that we obtained these results while our method has less parameter to tune (3 parameters) compared with [10] (4 parameters) and [1] (5 parameters).

5. CONCLUSION AND FUTURE WORK

We showed how to encode the star-shape prior into a continuous variational framework using directional derivatives to better model the cervical cell segmentation problem. To address the cell overlapping aspect of the segmentation, we proposed a Voronoi energy term as a soft constraint to control how much cells can overlap. Our approach outperformed the recently proposed techniques in both accuracy and computational time using non-optimized MATLAB code. There are at least two directions to extend this work: 1) preparing the method for real-time batch processing using GPU implementation, and 2) improving the boundaries in the dense and highly overlapping regions as the segmentation boundaries in such regions are still not very accurate.

6. REFERENCES

[1] Z Lu, G Carneiro, and AP Bradley, "Automated nucleus and cytoplasm segmentation of overlapping cervical cells," in *MICCAI*, pp. 452–460. 2013.

[2] ME Plissiti, C Nikou, and A Charchanti, "Automated detection of cell nuclei in pap smear images using morphological reconstruction and clustering," *IEEE TITB*, vol. 15, no. 2, pp. 233–241, 2011.

[3] SF Yang-Mao, YK Chan, and YP Chu, "Edge enhancement nucleus and cytoplast contour detector of cervical smear images," *IEEE TSMC*, vol. 38, no. 2, pp. 353–366, 2008.

[4] K Li, Z Lu, W Liu, and J Yin, "Cytoplasm and nucleus segmentation in cervical smear images using radiating gvf snake," *Patt. Recog.*, vol. 45, no. 4, pp. 1255–1264, 2012.

[5] A Gençtav, S Aksoy, and S Önder, "Unsupervised segmentation and classification of cervical cell images," *Patt. Recog.*, vol. 45, no. 12, pp. 4151–4168, 2012.

[6] A Kale and S Aksoy, "Segmentation of cervical cell images," in *ICPR*, 2010, pp. 2399–2402.

[7] N Phansalkar, S More, A Sabale, and M Joshi, "Adaptive local thresholding for detection of nuclei in diversity stained cytology images," in *ICCSP*, 2011, pp. 218–220.

[8] O Veksler, "Star shape prior for graph-cut image segmentation," in *ECCV*, pp. 454–467. 2008.

[9] AGC Bianchi DM Ushizima and CM Carneiro, "Segmentation of subcellular compartiments combining superpixel representation with voronoi diagrams," in *Overlapping Cervical Cytology Image Segmentation Challenge - IEEE ISBI*, pp. 1–2. 2014.

[10] MS Nosrati and GHamarneh, "A variational approach for overlapping cell segmentation," in *Overlapping Cervical Cytology Image Segmentation Challenge - IEEE ISBI*, pp. 1–2. 2014.